

COVERAGE AND DENSITY OF A LOW POWER, LOW DATA RATE, SPREAD SPECTRUM WIRELESS SENSOR NETWORK FOR AGRICULTURAL MONITORING

Louise H. Crockett, Eugen Pfann and Robert W. Stewart

Department of Electronic and Electrical Engineering, University of Strathclyde,
204 George Street, Glasgow, Scotland, U.K. G1 1XW.
Email: louise.crockett@eee.strath.ac.uk

ABSTRACT

A physical layer specification for a low power, low complexity, low data rate sensor network suitable for agricultural monitoring is investigated. Code division multiple access (CDMA) with high processing gain is used to facilitate transmission powers which comply with the Ultra Wide Band (UWB) spectral mask, and this permits physically small nodes with limited energy storage capacity. The interference arising from each node is calculated, and it is shown that for the investigated scenario and specification, an aggregate data rate of 2 bytes per minute and a node population of approximately 1000 can be supported at distances up to a few kilometres from the central node, with less than 0.2% chance of failure due to multiple access interference.

1. INTRODUCTION

SENSOR network technology is currently a very active research area, and various communications strategies have been investigated for addressing the problems associated with different network scenarios. There are many potential applications for sensor networks, and correspondingly their key characteristics (data rate, density, range, physical size, etc.) differ greatly [1,2,3].

In this paper, we consider a low complexity network in which nodes are of extremely small physical size and must consume very little power. They are required to monitor the wellbeing of livestock and relay the information back to a central collection point, as shown in Figure 1. Hence data rate requirements are modest, and an aggregate of a few bytes per minute is sufficient. The sensing nodes are unable to receive outward transmissions and consequently no synchronization exists in the network, however the central collecting node (CCN) is equipped with the resources to receive multiple asynchronous transmissions.

The key objective is to achieve a communication strategy which minimizes the complexity and transmit power of the sensing nodes, so that their battery life may be maximized. This is particularly important given the small dimensions required, and the resulting limit on energy storage capacity. It is assumed that the CCN is not energy limited.

The design goals outlined here lend themselves to comparison with the Global Positioning System (GPS) [4], in which a large processing gain is applied to the 50bps data broadcast by each satellite, thereby allowing the signal to

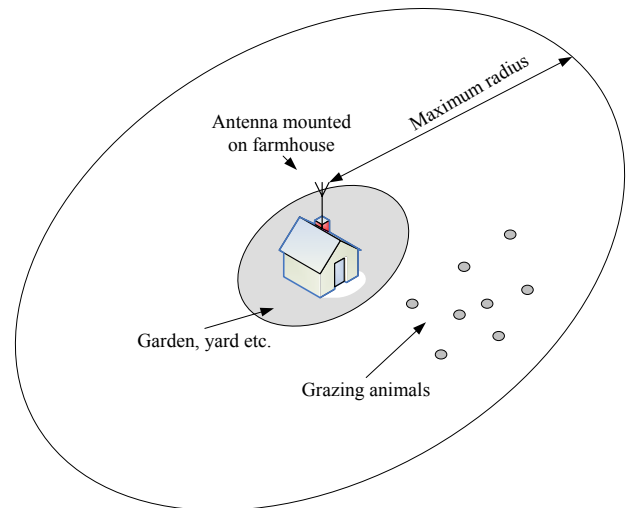


Figure 1 - Sensor network deployed for monitoring of farm animals be recovered from well below the noise floor.

Likewise, spread spectrum modulation can be applied to this simple sensor network. Doing so allows for the transmit power of the sensing nodes to be reduced, at the expense of additional digital signal processing in the receiver, and for the runtime to be extended as a result. CDMA is suitable for a number of reasons: firstly, the use of suitable spreading codes ensures that sources can be uniquely identified; secondly, the CCN can receive from several sources simultaneously; and thirdly, the burden of sensing the channel prior to commencing transmission is avoided, thus allowing node complexity and power consumption to be minimized.

This contribution aims to investigate the relationships between maximum node population, coverage, and transmission range for this simple low power, low data rate CDMA system, and to recommend a suitable design.

2. SYSTEM REQUIREMENTS

2.1 Topology

Nodes are spread randomly over an area of farmland surrounding the CCN. It is assumed that some nodes exist beyond the maximum transmission distance, but that transmissions from these nodes can still contribute interference. The minimum distance to the nearest animal implies a

node-free zone around the CCN.

As established in later sections of the paper, the permissible number of active nodes is constrained by the interference introduced by each source, and varies according to distance. Some degree of near-far effect is expected, and this is seen to reduce the maximum node population.

2.2 Communication System Design Parameters

Given the requirement of the system to collect slowly changing health data, an aggregate of 2 bytes per minute is sufficient to convey such measures as body temperature and heart rate.

A carrier frequency is chosen within the UWB band, which extends from 3.1GHz to 10.6GHz. A radio frequency which is “quiet” in the context of a rural outdoor scenario should be chosen. Therefore, frequencies designated for applications such as satellite communications and aviation should be avoided.

A further consideration is that, to minimize path loss, the frequency should be as low as possible; however a higher frequency is preferred in order to minimize antenna dimensions, which is important when physically small nodes are desired. A compromise of 7GHz has been chosen.

An upper limit on transmit power exists according to the UWB spectral mask, which permits transmit power spectral densities of up to -41.25dBW/MHz. Therefore the transmit power is limited according to the bandwidth chosen. In this analysis, a bandwidth of 2.046MHz is assumed, which limits the transmit power to -38.14dBW, or 153.45μW.

The channel considered is AWGN only. A free space path loss model is assumed, i.e.

$$path\ loss = \left(\frac{\lambda}{4\pi d} \right)^2$$

3. GPS SPREADING

The coarse acquisition (C/A) code for civil GPS is transmitted at 1.57542GHz in the L1 band [5]. 50bps data is spread by a factor of 20460 to a 1.023MHz bandwidth.

The spreading scheme repeats a 1023-chip Gold code 20 times for each data bit. During initial timing acquisition, correlation takes place over one Gold code period (i.e. 1023 chips, or 1/20th of a bit period), and once synchronization is achieved, the correlation is expanded to a full bit period (20460 chips). The code length is different from the processing gain, and it is denoted by F .

A typical received signal power is around -157.5dBW, approximately 19dB below the noise floor [6]. The processing gain is

$$10\log_{10}(20460) = 43.1\text{dB}$$

which results in a post-correlation SNR of approximately 24dB. The signal is recovered from the autocorrelation peaks on correlating with the desired code.

It is informative to summarize the power budget for GPS, and to map it to the proposed system.

Note that in both cases, the bandwidth is 2MHz and the

noise temperature is assumed to be 513K [6], which includes both thermal and receiver noise.

TABLE I
POWER BUDGET FOR GPS MAPPED TO THE PROPOSED SENSOR NETWORK

	GPS	Sensor Network
SNR (post-correlation)	24dB	24dB
Processing Gain	43.1dB	43.1dB
SNR (pre-correlation)	-19.1dB	-19.1dB
Noise floor	-138.5dBW	-138.5dBW
<i>Bandwidth</i>	2MHz	2MHz
<i>Noise temperature</i>	513K	513K
Received Power	-157.6dBW	-157.6dBW
Path loss	-182.41dB	-119.46dB
<i>Distance</i>	20,000,000m	3205m
<i>Carrier frequency</i>	1.57542GHz	7GHz
Atmospheric attenuation	-2dB	0dB
Transmit Power	26.81dBW	-38.14dBW

Table I shows that 3205m is the maximum range at which a post-correlation SNR of 24dB is achieved for maximum transmit power, i.e. -38.14dBW, in zero interference conditions. Later in the paper, interference will be considered and this requirement will be revised.

Assuming equal transmit power, a 1-bit ADC causes a greater reduction in transmission distance than multi-bit ADCs (due to its 3.5dB SNR loss [6]), but is still an attractive option because active gain control is not required and matched filter complexity can be minimized.

Incorporating the 3.5dB loss in the power budget given in Table I results in a maximum range of 2142m.

4. GOLD CODE SPREADING

Gold codes [7] are pseudo-orthogonal codes which are easily generated from linear feedback shift registers (LFSRs). The method involves creating a preferred pair of maximal length sequences (m-sequences) from two LFSRs, and then forming a set of Gold codes by combining time shifted versions of these m-sequences.

Gold code generators can be implemented at very low hardware cost, as shown in Figure 2, and hence are suitable for the application considered in this paper.

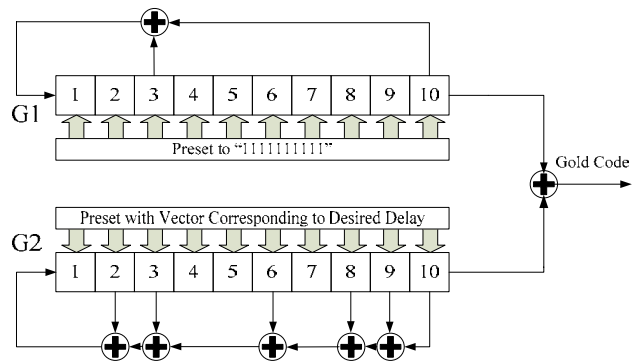


Figure 2 - Gold Code Generator (1023 chips)

Gold codes have well characterized cross correlation properties [8], which is useful when quantifying the cross correlation interference (CCI) between codes. This parameter helps to determine the number of nodes that can be supported simultaneously, given the interference they each contribute.

Specifically, the periodic cross-correlation of any two Gold codes from a set results in three possible values. These can be determined algebraically, as detailed in [8].

Figure 3(a) illustrates the characteristic 3-valued periodic cross correlation function, which occurs when there is no transition in the interfering data source, and displays regular properties. Figure 3(b) shows the odd cross correlation, which results when a transition is present in the interfering data.

As the system is asynchronous, cross correlation should be evaluated on a continuous time basis. The approximate CCI power may be found experimentally by upsampling the codes by a factor of U , prior to cross correlating.

For the periodic case,

$$\overline{P_{CC_{even}}} = \frac{1}{UF} \sum_{f=0}^{UF-1} \theta_{x,y} [f]^2$$

and for the odd case,

$$\overline{P_{CC_{odd}}} = \frac{1}{UF} \sum_{f=0}^{UF-1} \hat{\theta}_{x,y} [f]^2$$

where $\theta_{x,y}$ and $\hat{\theta}_{x,y}$ are the periodic and odd cross correlation functions defined in [8], and f denotes samples from the spreading sequence of length F . The results reported below are based on the chosen value of $U = 10$.

With balanced random data, odd and periodic cross correlation are equally probable, but in the considered application this is true only $1/20^{\text{th}}$ of the time, due to the repetition of spreading codes 20 times per bit period. Periodic correlation occurs otherwise. The overall CCI power is therefore

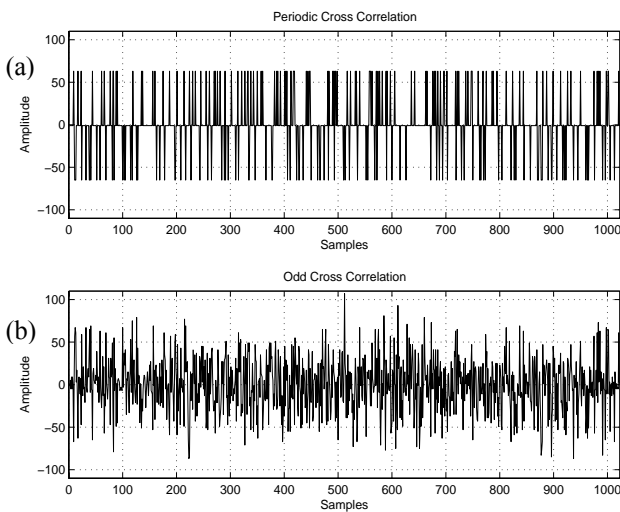


Figure 3 - (a) Periodic cross correlation, (b) Odd cross correlation

$$\overline{P_{CC}} = \frac{19.5\overline{P_{CC_{even}}} + 0.5\overline{P_{CC_{odd}}}}{20}$$

which has a numerical value of 686.29 for the chosen oversampling ratio and Gold code family.

Finally, expressed normalized to the auto correlation peak,

$$CCI = 10 \log_{10} \left(\frac{\overline{P_{CC}}}{F^2} \right) = -31.83dB$$

5. ANALYSIS OF SYSTEM PARAMETERS

CCI information is useful because it quantifies the relative interference power introduced by each node, and assists in determining the overall level of noise (N) plus interference (I) in the system for a given number of active nodes. Multiple Access Interference (MAI) power is the CCI weighted by the power of interferers, and directly influences $E_b/(N_0+I_0)$, and hence the bit error rate (BER) of the system.

I_0 represents the interference normalized by bandwidth, and is dependent on the number of nodes in the system. It may be omitted from the equation when interference is far outweighed by noise, but in a network comprising tens or even hundreds of nodes, interference can be significant and I_0 should not be discounted.

It is shown in [9] that $E_b/(N_0+I_0)$ can be related to the processing gain (G_p) and received signal power (S),

$$\frac{E_b}{N_0 + I_0} = \frac{S/R}{(N+I)/W_{SS}} = \frac{G_p S}{(N+I)} \quad (1)$$

where R is the bit rate and W_{SS} is the spread spectrum bandwidth. The minimum level of $E_b/(N_0+I_0)$ is defined by the desired BER according to

$$P(e) = \frac{1}{2} \left[1 - \operatorname{erf} \left(\sqrt{\frac{E_b}{N_0 + I_0}} \right) \right]$$

where $P(e)$ denotes the probability of error. It is assumed that a BER of $1e^{-4}$ is required, and this yields

$$\varepsilon = \frac{E_b}{N_0 + I_0} \geq 6.916$$

where ε is introduced to represent $E_b/(N_0+I_0)$.

5.1 Perfect Power Control Analysis

Equation (1) may be simplified by assuming that interference power, I , is equal to the received signal power multiplied by $M-1$, where M is the total number of active nodes in the system. This implies that the power received from all nodes is equal, i.e. equidistant nodes or perfect power control. Although both are infeasible in practice, assuming equal received power is useful for initial analysis.

$$\varepsilon = \frac{G_p S}{N + S(M-1)} = \frac{G_p}{N/S + (M-1)} \quad (2)$$

Equation (2) infers that the entire signal power of each other node causes interference, which has been shown not to be true in this case. Having calculated the MAI caused by a single source in the previous section, this equation can be modified to express more accurately the interfering power. A factor is introduced,

$$K = G_p \frac{\overline{P_{CC}}}{F^2}$$

and using the value of $\overline{P_{CC}}$ found in Section 6, K is 13.42.

Additionally, N is replaced by N' , which includes the noise degradation of the analogue to digital conversion (ADC) stage. The post-ADC noise power is given by

$$N' = \frac{N}{A}$$

where A reflects the relative quantization noise power of the ADC (-3.5dB in this case). Hence (3) follows from (2).

$$\varepsilon = \frac{G_p}{N'/S + K(M-1)} \quad (3)$$

As the noise floor, bandwidth and transmit power are all fixed, it is clear that the received signal power, S , is a function of distance from the CCN. In the first instance this distance is assumed constant for all nodes. Substituting the simple path loss model and rearranging provides the maximum transmission distance for successful reception, d_{max} .

$$d_{max} = \frac{\lambda}{4\pi \times \sqrt{\frac{N'}{P_{tx} \left(\frac{G_p}{\varepsilon} - K(M-1) \right)}}$$

5.2 No Power Control: Mean Path Loss Analysis

Clearly the previous section represents the best case, as all received signals are of equal power and the near-far problem does not occur. However, in a realistic scenario it cannot be assumed that all nodes are equidistant. A more general expression for (2) is derived, which takes account of the powers in each received signal. The desired source has the subscript I , and the others are indexed from 2 to M .

$$\varepsilon = \frac{G_p \cdot S_I}{N' + K \cdot \sum_{i=2}^M S_i} \quad (4)$$

In analysing the average case, it is useful to determine the mean or expected received signal power of interferers, which are assumed to be uniformly randomly distributed. The expectation of mean received signal power is derived using a radius Probability Density Function (PDF).

$$PDF(r) = \frac{2r}{d_{int}^2 - d_{min}^2}$$

where consideration of interferers is limited to the area bounded by d_{min} , and d_{int} . The parameter d_{min} is the radius around the farmhouse within which animals are absent, and d_{int} is the distance at which the despread interference arising from a source becomes insignificant compared to noise. "Insignificant" is defined as contributing a power 20dB below the noise floor.

$$d_{int} = \frac{\lambda}{4\pi \sqrt{\frac{N'}{100K P_{tx}}}}$$

The expected path loss of interfering nodes, $E(\alpha)$, is found,

$$E(\alpha) = \int_{d_{min}}^{d_{int}} \left(\frac{\lambda}{4\pi r} \right)^2 PDF(r) dr$$

along with $E(M)$, the expectation of transmitting nodes in the same area,

$$E(M) = \gamma\pi(d_{int}^2 - d_{min}^2)$$

which is based on the intensity, γ , of the Poisson Point Process (PPP) [10] used to model the placement of transmitting nodes, with γ given in nodes per m^2 .

Equation (4) is amended to reflect the average power of interferers,

$$\varepsilon = \frac{G_p S_I}{N' + K E(M) S_{mean}}$$

where S_I represents the received power of the desired source, and S_{mean} is the expected received power of individual interferers (i.e. $P_{tx}E(\alpha)$). Therefore, in average conditions, the maximum distance at which reception is successful is

$$d_{max} = \frac{\lambda}{4\pi \times \sqrt{\frac{\varepsilon}{G_p P_{tx}} (N' + K E(M) P_{tx} E(\alpha))}} \quad (5)$$

and the population of transmitting nodes enclosed in the resulting coverage ring is

$$M_{tx} = \gamma\pi(d_{max}^2 - d_{min}^2) \quad (6)$$

6. SIMULATION RESULTS

In this section, the variation of the number of transmitting nodes within the coverage area, M_{tx} , with maximum transmission distance, d_{max} , is shown for different values of the inner radius, d_{min} . These trends are considered for average conditions, and correspond to Equations (5) and (6).

Considering the agricultural context, d_{min} refers to the node-free area around the farmhouse where the antenna is mounted, and therefore it is reasonable to assume d_{min} might

be a few tens of metres. Using the parameters stated in Section 4, d_{min} is found to be 8.677km.

The maximum number of transmitting nodes within the coverage area is evaluated for $d_{min} = 10m, 30m, 50m,$ and $70m,$ and plotted in Figure 4. The graph illustrates that, in general, fewer active users can be supported as the required coverage area increases: hence the intensity of the PPP must be reduced if a larger coverage area is required. It is also notable that the constraints on transmitting node population and maximum distance lessen as the prohibited area expands. This is due to the reduction in the dynamic range of received power, and hence the Near Far Effect.

As an example, the region between 50m and 6.7km from the CCN could support up to 6 active nodes. Considering the data transfer requirement of 16 bits per minute, and available data rate of 50 bits per second, the probability of transmission, $P(tx)$, is 0.0053. Therefore, if node transmission activity is modeled by a Poisson distribution with mean 5 and probability 0.0053, a total node deployment of 943 may be supported within the coverage area.

The probability of packet failure, $P(pf)$ for the 16 bit packet is given by

$$P(pf) = 1 - (1 - P(e))^l = 1 - (1 - 1e^{-4})^{16}$$

where uncoded data is assumed, and l is the packet length in bits, which evaluates to $1.6e^{-3}$.

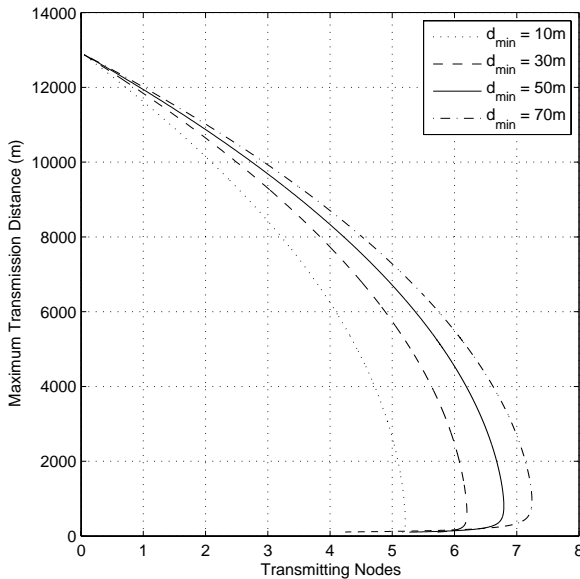


Figure 4 - Maximum distance versus active node population

7. CONCLUSIONS

This paper has proposed and evaluated a suitable CDMA physical layer for a low power, low data rate wireless sensor network capable of monitoring the wellbeing of farm animals. Through analysis of multiple access interference, it has been shown that a UWB-compliant transmit power can be used, and that the cost and complexity of the transmitter

hardware is modest, which implies low levels of power dissipation in the remote sensor nodes.

Relationships between the key parameters of $E_b/(N_0+I_0)$, transmission distance and transmitting node population were established, and a realistic scenario was evaluated. In this example, it was found that placing the receiver to reduce the near far effect to a tolerable level resulted in up to 943 sensor nodes being accommodated within 6.7km of the central node, with less than a 0.2% chance of packet error due to multiple access interference.

REFERENCES

- [1] M. Kuorilehto, M. Hannikainen, and T. D. Hamalainen, "A Survey of Application Distribution in Wireless Sensor Networks," *EURASIP Journal on Wireless Communications and Networking*, vol. 5, issue 5, pp. 774-788, October 2005.
- [2] K. Romer and F. Mattern, "The Design Space of Wireless Sensor Networks," *IEEE Wireless Communications Magazine*, Dec. 2004.
- [3] P. Sikka et al, "Wireless Sensor and Actuator Networks on the Farm," *Proceedings of the 5th International Conference on Information Processing in Sensor Networks*, Nashville, USA, 2006.
- [4] "USNO Navstar Global Positioning System," available: <http://tycho.usno.navy.mil/gpsinfo.html>
- [5] E. D. Kaplan and C. J. Hegarty, *Understanding GPS Principles and Applications*. MA: Artech House, 2006, ch. 4.
- [6] M. S. Braasch and A. J. Van Dierendonck, "GPS Receiver Architectures and Measurements," *IEEE Proceedings*, vol. 87, no. 1, January 1999
- [7] E. H. Dinan and B. Jabbari, "Spreading Codes for Direct Sequence CDMA and Wideband Cellular Networks," *IEEE Communications Magazine*, Sept. 1998.
- [8] D. V. Sarwate and M. B. Pursley, "Crosscorrelation Properties of Pseudorandom and Related Sequences," *IEEE Proceedings*, vol. 68, issue 5, May 1980, pp. 593-619.
- [9] B. Sklar, *Digital Communications: Fundamentals and Applications*. NJ: Prentice Hall, 2001, pp. 777-779.
- [10] D. Stoyan, W. S. Kendall and J. Mecke, *Stochastic Geometry and Its Applications*, Wiley, 1987.